Published OnlineFirst August 2, 2006; DOI: 10.1158/1541-7786.MCR-06-0060

Protein Expression Profiling Identifies Cyclophilin A as a Molecular Target in Fhit-Mediated Tumor Suppression

Shuho Semba and Kay Huebner

Comprehensive Cancer Center and Department of Molecular Virology, Immunology, and Medical Genetics, Ohio State University, Columbus, Ohio

Abstract

Loss of fragile histidine triad (Fhit) expression is often associated with human malignancies, and Fhit functions as a tumor suppressor in controlling cell growth and apoptosis, although specific signal pathways are still undefined. We have used a proteomic approach to define proteins in the Fhit-mediated tumor suppression pathway. Because substitution of Tyr^{114} (Y114) with phenylalanine (Y114F) diminishes Fhit functions, we did protein expression profiling to identify proteins differentially expressed in Fhit-negative H1299 lung cancer cells infected with wild-type (Ad-*FHIT*-wt) and Y114 mutant *FHIT*-expressing (Ad-*FHIT*-Y114F) adenoviruses. Among 12 distinct proteins that exhibited 4-fold differences in expression on comparison of the two infected cell lysates, cyclophilin A, the intracellular reporter of the immunosuppressive drug cyclosporine A, showed a remarkably decreased protein level in cells infected with Ad-*FHIT*-wt versus Ad-*FHIT*-Y114F. Conversely, loss of Fhit expression resulted in increased cyclophilin A expression in mouse tissues and cell lines. Restoration of Fhit expression led to down-regulated cyclophilin A protein expression and subsequently prevented cyclophilin A–induced up-regulation of cyclin D1, Cdk4, and resultant cell cycle progression (G_1-S transition), which was independent of Ca^{2+}/calmodulin-dependent kinase inhibitor, KN-93. Interestingly, Fhit down-modulation of phosphatase activity of calcineurin, which controls cyclin D1/Cdk4 activation, was reversed by cyclophilin A treatment in a concentration-dependent manner, a reversal that was inhibited by additional cyclosporine A treatment. Thus, cyclophilin A is a downstream target in Fhit-mediated cessation of cell cycle progression at late G_1 phase. Elucidation of the protein effectors of Fhit signaling may lead to identification of targets for lung cancer therapy. (Mol Cancer Res 2006;4(8):529–38)

Introduction

Loss of heterozygosity involving markers on the short arm of chromosome 3, a region encompassing several tumor suppressor genes, is one of the earliest and most frequently acquired genetic changes occurring in the pathogenesis of lung cancer (1). The *fragile histidine triad* (*FHIT*) gene spans the most active common fragile site in the human genome, *FRA3B* (3p14.2), which is frequently involved in biallelic loss, genomic rearrangement, and cytogenetic abnormalities in lung cancer (2-4). Dysregulation of Fhit expression by deletions at the *FHIT* locus, or promoter hypermethylation, was frequently detected not only in cancers but also in premalignant lesions (5-7).

Over the last several years, evidence confirming tumor suppressor functions of Fhit has accumulated: $Fhit^{-/-}$ and $Fhit^{+/-}$ mice exhibit increased susceptibility to spontaneous tumors and deletion of a *Fhit* allele in mice enhances sensitivity to carcinogens, *N*-nitrosomethylbenzylamine and dimethylnitrosoamine (8-11); deficiency of Fhit protein decreases sensitivity to DNA-damaging agents, such as mitomycin C, UVC, and ionizing radiation (12, 13). Furthermore, overexpression of *FHIT* by adenoviral gene delivery effectively suppressed cell growth and induced caspase-dependent apoptosis in *in vitro* and *in vivo* experiments (14-17). Thus, Fhit is considered to play an important role in tumorigenesis, and *FHIT* gene therapy may be a useful clinical approach in treatment of human cancers and prevention of tumor development (18). However, the mechanism through which Fhit induces cell cycle arrest and apoptosis in cancer cells requires further elucidation. Recently, to investigate the biological significance of the Fhit amino acid sequence $DSIY^{114}EEL$, the consensus target of phosphorylation by Src tyrosine kinase family members (19), site-directed mutagenesis at Tyr^{114} (Y114) and mRNA expressing profiling were done after adenovirus-mediated delivery of wild-type and mutant *FHIT*; it was shown that expression of *survivin*, a member of the inhibitor of apoptosis protein family, was decreased only by wild-type Fhit possibly as a result of inactivation of the phosphatidylinositol 3-kinase/Akt signaling pathway (20).

As another approach to defining Fhit signal pathways, we herein used protein expression profiling to search for new effector proteins. Proteomics is advantageous for analyzing the complete complement of proteins expressed by a biological

Received 3/2/06; revised 5/18/06; accepted 6/5/06.
Grant support: National Cancer Institute/NIH, USPHS grant CA77738 (K. Huebner) and Ohio State University Comprehensive Cancer Center.
The costs of publication of this article were defrayed in part by the payment of page charges. This article must therefore be hereby marked advertisement in accordance with 18 U.S.C. Section 1734 solely to indicate this fact.
Note: Supplementary data for this article are available at Molecular Cancer Research Online (http://mcr.aacrjournals.org/).
Requests for reprints: Kay Huebner, Comprehensive Cancer Center and Department of Molecular Virology, Immunology, and Medical Genetics, Ohio State University, Room 455C, Wiseman Hall, 410 West 12th Avenue, Columbus, OH 43210. Phone: 614-292-4850; Fax: 614-292-3312. E-mail: kay.huebner@osumc.edu

doi:10.1158/1541-7786.MCR-06-0060

Published OnlineFirst August 2, 2006; DOI: 10.1158/1541-7786.MCR-06-0060

system in response to various stimuli and/or under different physiologic or pathologic conditions, because examining changes in the proteome offers insight into cellular and molecular mechanisms that cannot always be obtained through genomic or RNA expression analyses. Therefore, based on evidence that Y114 mutant Fhit proteins do not exhibit tumor suppression activity, we reasoned that a display of the proteins differentially expressed in cells overexpressing wild-type or Y114 mutant Fhit protein could uncover novel molecular targets that would be activated or inactivated during Fhit-mediated tumor suppression.

Results

Biological Significance of Fhit Y114 for Tumor Suppressive Activity

To identify pathways through which Fhit induces tumor-suppressing activity, we exploited the biological differences between wild-type and mutant *FHIT* adenoviruses (20). For analysis of the effects of recombinant Fhit proteins, H1299 human lung cancer cells were infected with Ad-*FHIT*-wt and Ad-*FHIT*-Y114F, respectively. Because the adenoviral vector used in this study was designed to express green fluorescent protein (GFP) simultaneously with the gene of interest, >95% viral infectivity 24 hours after infection was confirmed by detecting GFP by fluorescent microscopy (data not shown). Fhit-Y114F protein showed a slightly lower gel mobility on immunoblots compared with Fhit-wt protein (Fig. 1A, *a*). Ad-*FHIT*-wt effectively suppressed cell growth and viability in a multiplicity of infection (MOI)–dependent manner, whereas Ad-*FHIT*-Y114F did not show a significant growth-inhibitory effect compared with the control Ad-*GFP* virus (Fig. 1A, *b*). The population of cells in sub-G_1 and active (cleaved) caspase-3-positive cells were dramatically increased by overexpression of Fhit-wt but not Fhit-Y114F (Fig. 1B). We also analyzed bromodeoxyuridine (BrdUrd) incorporation to assess effect of Fhit proteins on cell cycle progression at late G_1 and found that Fhit-wt effectively suppressed the G_1-S transition, but Fhit-Y114F was less effective (Fig. 1C).

Protein Expression Profiles in H1299 Cells Infected with Ad-FHIT-wt and Ad-FHIT-Y114F

Based on the difference in biological effects between wild-type and Y114 mutant *FHIT*-expressing adenoviruses, two-dimensional PAGE was done for proteins extracted from cells infected with Ad-*FHIT*-wt or Ad-*FHIT*-Y114F (MOI 25) on immobilized pH gradient strips of pH 3 to 10. To avoid contamination with apoptotic cells that occurs at 4 to 7 days postinfection, the infected H1299 cells were collected after 72 hours. Overall, the protein spot patterns of individual lysates were almost equivalent; the levels of exogenous recombinant Fhit and GFP proteins overexpressed in H1299 cells were almost equivalent, whether expressing wild-type or Y114 mutant, indicating equivalent infectivity of each virus (Fig. 2A). After normalization of background proteins and artifacts, 12 distinct proteins were identified from the spots that exhibited at least 4-fold differences by matrix-associated laser desorption/ionization time of flight (MALDI-TOF) and mass spectrometry (MS; Fig. 2B). The theoretical and observed molecular weights and isoelectric point, Est's *Z* score, and expression trend (Ad-*FHIT*-wt versus Ad-*FHIT*-Y114F) as well as known functional significance for these proteins are summarized in Table 1.

Among the proteins identified by MS, altered expression of Annexin A2 (ANXA2), cyclophilin A, heat shock protein 70 (HSP70) isoform 1, and carbonic anhydrase II (CAII) was assessed by Western blot analyses. Increased ANXA2 expression and decreased cyclophilin A expression were detected in cells infected with Ad-*FHIT*-wt in accordance with the results of proteome analysis; however, there was no significant difference in HSP70 isoform 1 and CAII expression (Fig. 3A, *a*; Supplementary Fig. S1A, a). We also assessed the expression levels of these proteins in $Fhit^{+/+}$ and $Fhit^{-/-}$ cells *in vitro* and *in vivo*. Mouse kidney cells lacking Fhit showed increased cyclophilin A levels (Fig. 3A, *b*), whereas there was no difference between $Fhit^{+/+}$ and $Fhit^{-/-}$ cells in protein levels of ANXA2, HSP70, and CAII (Supplementary Fig. S1A, b). After wild-type and mutant *FHIT* viral infection, the level of *cyclophilin A* mRNA expression was slightly decreased (Fig. 3A, *c*), although *GFP* viral infection did not cause a decrease (data not shown). Because the difference in *cyclophilin A* mRNA level, especially at 72 hours, was not significant when comparing cells infected with Ad-*FHIT*-wt and Ad-*FHIT*-Y114F (Fig. 3A, *c*), it seems unlikely that the observed decrease in *cyclophilin A* mRNA could account for the reduction in protein level observed only after Ad-*FHIT*-wt infection. Interestingly, nuclear localization of cyclophilin A was effectively suppressed by infection of Ad-*FHIT*-wt, which was not significant in the cells infected with Ad-*FHIT*-Y114F (Fig. 3B). Similarly, we also confirmed that loss of Fhit expression in bronchial cells and lung tumors caused significantly higher levels of cyclophilin A expression in mouse tissues (Fig. 3C). No significant difference was found in the levels of ANXA2, HSP70 isoform 1, or CAII (Supplementary Fig. S1B).

To determine the mechanism(s) that could contribute to Fhit down-regulation of cyclophilin A expression, we next investigated altered levels of cyclophilin A in the presence of cycloheximide. When translation of genes was inhibited by cycloheximide, reduced levels of cyclophilin A expression were observed only in H1299 cells overexpressing Fhit-wt (Fig. 3D, *a*). In addition, by treatment with proteasome inhibitor, Z-Leu-Leu-Leu-al (MG132), Fhit-mediated degradation of cyclophilin A was suppressed (Fig. 3D, *b*), suggesting that Fhit overexpression may affect stability of cyclophilin A protein.

Fhit Inhibits Cyclophilin A–Mediated Calcineurin Activity and G_1-S Transition

Cyclophilin A is also known to promote calcineurin-dependent G_1-S transition by up-regulating cyclin D1 expression and Cdk4 activity in late G_1 phase (21-23). We confirmed up-regulation of both cyclin D1 and Cdk4 expression by cyclophilin A (10 ng/mL) treatment 60 minutes after exposure in synchronized H1299 cells; however, in the cyclophilin A–mediated G_1-S transition, there was no significant change in $p21^{WAF1}$ expression levels (Fig. 4A). We thus investigated the effect of Fhit on cyclophilin A effects in the progression of cell

Published OnlineFirst August 2, 2006; DOI: 10.1158/1541-7786.MCR-06-0060

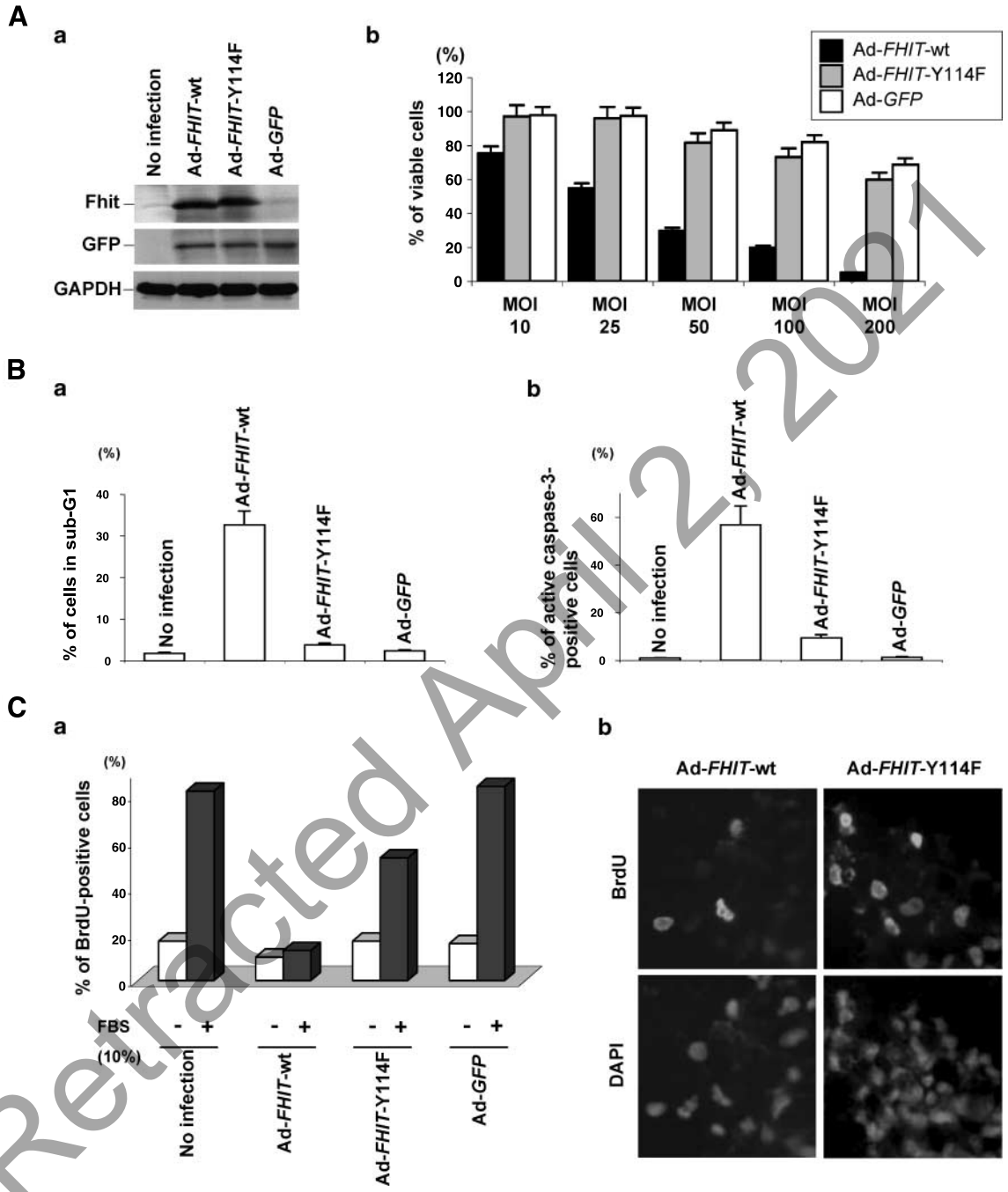

FIGURE 1. Characterization of Ad-*FHIT*-wt-infected and Ad-*FHIT*-Y114F-infected H1299 human lung carcinoma cells. **A.** Cell viability test after Ad-*FHIT*-wt and Ad-*FHIT*-Y114F infection. **a**, Western blot of recombinant Fhit proteins. Fhit-Y114F protein showed a lower gel mobility than Fhit-wt. As control of infectivity of viruses and protein loading, antisera against GFP and GAPDH were used. **b**, wild-type Fhit protein suppressed cell viability in a MOI-dependent manner. Cells were infected with individual adenoviruses and incubated for 120 hours. **B.** Percentage of cells in sub-G_1 DNA (**a**) and positive for active caspase-3-positive cells (**b**). **C.** BrdUrd incorporation after adenoviral recombinant *FHIT* gene delivery. **a**, cells were incubated in serum-free medium for 48 hours and then infected with individual adenoviruses 24 hours before treatment with BrdUrd in the presence or absence of fetal bovine serum (*FBS*). **b**, representative BrdUrd-positive cells after Ad-*FHIT*-wt and Ad-*FHIT*-Y114F infection.

cycle. H1299 cells were synchronized in serum-free medium for 48 hours and then infected with adenoviruses carrying wild-type and mutant *FHIT* 24 hours before cyclophilin A treatment. Because cyclophilin A has also been documented to activate cyclin D1 and Cdk4 in Ca^{2+}/calmodulin-dependent cell cycle regulation (21-23), we also used the Ca^{2+}/calmodulin-dependent kinase inhibitor KN-93 in the process of transitioning cells into S phase. Although KN-93 did not have pivotal effects to inhibit G_1-S transition induced by cyclophilin A in H1299 cells, the number of BrdUrd-positive cells was

Published OnlineFirst August 2, 2006; DOI: 10.1158/1541-7786.MCR-06-0060

significantly suppressed by wild-type Fhit expression (Fig. 4B). In support of these results, expression of cyclin D1 and Cdk4 was increased by cyclophilin A in the control cells and cells infected with Ad-*FHIT*-Y114F and Ad-*GFP* but not in cells infected with Ad-*FHIT*-wt (Fig. 4C).

Finally, we assessed calcineurin activity with or without cyclophilin A treatment. Results are illustrated in Fig. 5. Although phosphatase activity of calcineurin was down-regulated by Fhit-wt, addition of cyclophilin A allowed recovery of calcineurin phosphatase activity in a dose-dependent manner. Interestingly, when cells were treated with cyclosporine A, the effects of cyclophilin A tended to be suppressed in accordance with cyclosporine A concentration.

Discussion

Because loss of Fhit expression is an early event in development of many cancers and is associated with poor prognosis in some cancers, including lung and breast cancers (24-26), elucidation of the mechanism by which Fhit affects cell growth and tumorigenesis may identify diagnostic markers and therapeutic targets. Although differentially expressed genes in human lung cancers have been identified, few have been translated into protein markers that can aid in diagnosis and effective treatment. This study identified differentially expressed proteins in wild-type and mutant *FHIT*-expressing lung cancer cells; despite the minimal structural differences, the Fhit-wt protein induced apoptotic activity and cell cycle distribution effects not seen with Fhit-Y114F. Thus, we hypothesized that protein lysates from H1299 cells infected with these two viruses would be useful in protein expression profiling experiments to discover protein effectors of Fhit-mediated tumor-suppressing pathways. Although the approach of protein separation by two-dimensional PAGE coupled with protein identification by MALDI-TOF analysis has inherent limitations, we identified 12 proteins that were apparently differentially expressed in wild-type and Y114F mutant *FHIT*-infected H1299 human lung cancer cells. According to the biological evidence supporting Fhit tumor suppressor function, Fhit is likely to possess diverse functions in controlling cell proliferation, proapoptotic signaling, and sensitivity to DNA damage responses (5, 8), but protein effectors of these diverse

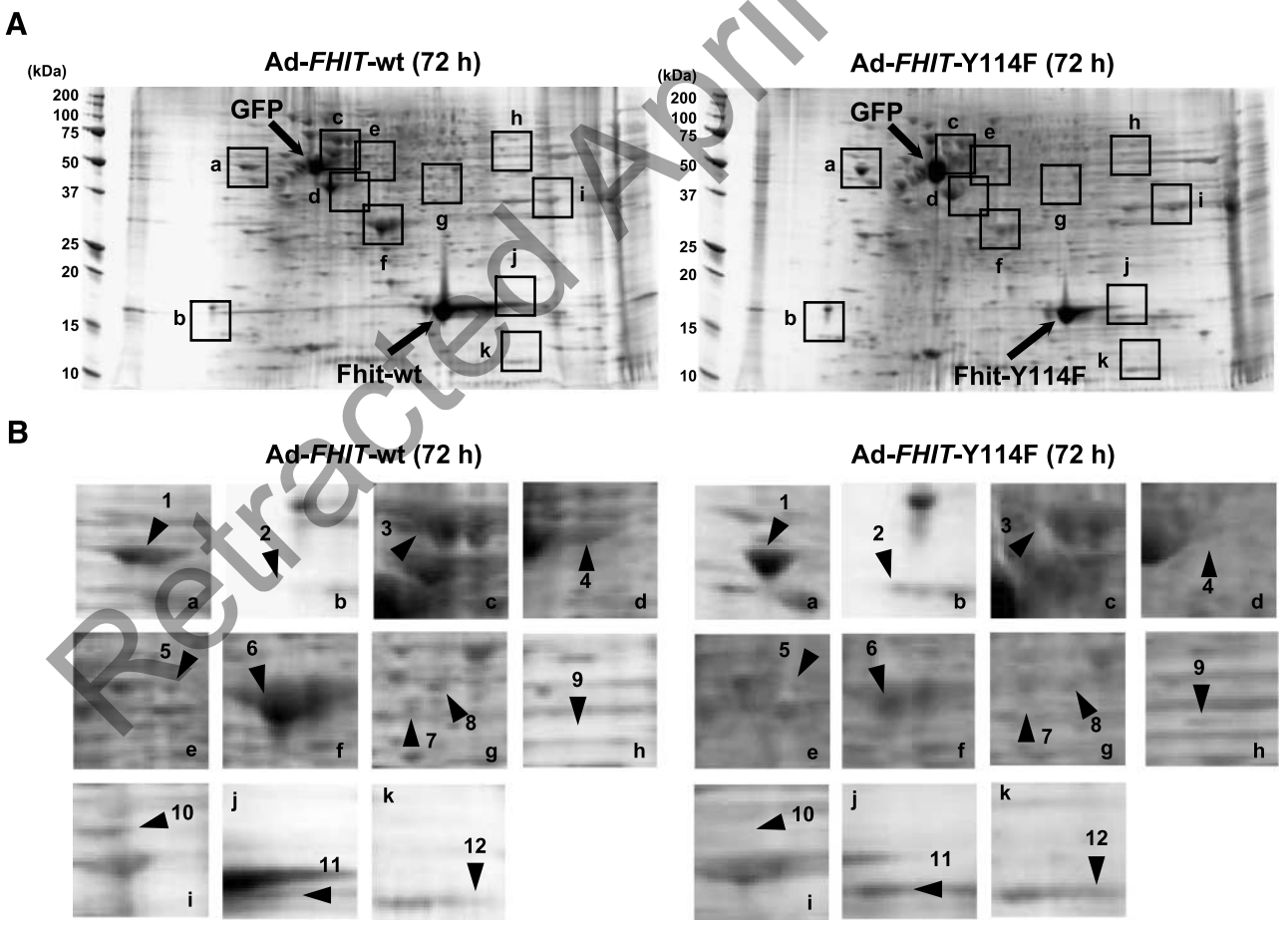

FIGURE 2. Two-dimensional PAGE images of proteins from H1299 cells infected with Ad-*FHIT*-wt or Ad-*FHIT*-Y114F. **A.** Full-size two-dimensional PAGE images. The cells were collected and lysed 72 hours after viral infection (MOI 25). Gels were stained with colloidal Coomassie blue. Recombinant adenovirus-derived Fhit and GFP proteins were confirmed by MS (*arrows*). Squares **a** to **k**, location of proteins differentially expressed (>4-fold). **B.** Magnified two-dimensional PAGE images of selected proteins. **a**, spot 1, calreticulin; **b**, spot 2, ubiquitin-conjugating enzyme E2H; **c**, spot 3, HSP70 isoform 1; **d**, spot 4, EIF4A; **e**, spot 5, ER60; **f**, spot 6, CAII; **g**, spot 7, HSP70 isoform 2; spot 8, keratin 7; **h**, spot 9, glutamate dehydrogenase 1; **i**, spot 10, ANXA2; **j**, spot 11, cyclophilin A; **k**, spot 12, T-cell receptor α chain.

Published OnlineFirst August 2, 2006; DOI: 10.1158/1541-7786.MCR-06-0060

Table 1. Differentially Expressed Proteins in H1299 Lung Cancer Cells Infected with Ad-*FHIT*-wt and Ad-*FHIT*-Y114F

Spot no.	Protein identity	Accession no.	MALDI-TOF coverage (%)	Protein size actual/expected (kDa)	Isoelectric point actual/expected	Est's *Z* score*	Protein expression Ad-*FHIT*-wt vs Ad-*FHIT*-Y114F†	Reported functions
Ca^{2+} binding/Ca^{2+} associated								
1	Calreticulin	NP_004334.1	42	46/48.29	4.3/4.3	2.16	Minus in wild-type	RNA binding
10	ANXA2	NP_001002858	48	36/38.79	9.0/7.7	2.30	Plus in wild-type	Ca^{2+}-dependent phospholipid binding
11	Cyclophilin A	NP_066953.1	64	16/18.09	8.1/8.1	2.43	Minus in wild-type	Immunophilin (cyclosporine A) binding
ATP binding								
3	HSP70, isoform 1 (70 kDa)	NP_006588.1	24	70/71.11	5.7/5.4	2.16	Plus in wild-type	ATP binding
7	HSP70, isoform 2 (42 kDa)	NP_694881	32	42/41.98	7.2/6.7	1.52	Plus in wild-type	ATP binding
4	Eukaryotic translation initiation factor 4A	NP_001407.1	40	42/46.36	5.9/5.3	2.43	Plus in wild-type	ATP-dependent helicase activity
Proteases and catalytic enzymes								
2	Ubiquitin-conjugating enzyme E2H	NP_003335.1	25	15/20.69	3.9/4.6	2.43	Present in mutant	Ubiquitin-protein ligase activity
5	ER60	S63994	34	58/57.18	6.4/6.0	1.67	Plus in wild-type	Protein disulfide-isomerase activity
6	CAII	NP_000058	36	29/29.10	6.4/6.9	2.43	Plus in wild-type	Reversible hydration of carbon dioxide
9	Glutamate dehydrogenase 1	NP_005262.1	44	61/61.72	8.2/7.8	2.08	Minus in wild-type	Synthesis and catabolism of glutamate
Others								
8	Keratin 7	NP_005547.3	26	48/51.43	7.2/5.4	2.43	Plus in wild-type	Cell structure/ Intermediate filament
12	T-cell receptor α chain	AAN12378.1	77	11/11.06	8.4/6.7	1.19	Minus in wild-type	Cellular defense/MHC protein binding

*A *Z* score is estimated when the search result is compared against an estimated random match population. *Z* score is the distance to the population mean in unit of SD. It also corresponds to the percentile of the search in the random match population. For instance, a *Z* score of 1.65 for a search means that the search is in the 95th percentile. In other words, there are ~5% of random matches that could yield higher *Z* scores than this search. The following is a list for *Z* score and its corresponding percentile in an estimated random match population: *Z* score 1.282, 90.0 percentile; *Z* score 1.645, 95.0 percentile; *Z* score 2.326, 99.0 percentile; *Z* score 3.09, 99.9 percentile.
†Proteins differentially expressed in H1299 cells infected with Ad-*FHIT*-wt and Ad-*FHIT*-Y114F (cutoff value, 4-fold).

functions have not been identified. We now report that cyclophilin A is a target protein suppressed by Fhit in the transition of the cells into S phase.

Recently, specific intracellular signaling pathways have been reported to be involved in Fhit-mediated tumor suppression. Inactivation of the phosphatidylinositol 3-kinase/Akt/survivin pathway by Fhit is also implicated in Fhit-mediated apoptosis signaling (20). We assessed previously the Atr-Chk1 pathway in response to mitomycin C, UVC, and ionizing radiation in Fhit-positive and Fhit-negative cells and found that Fhit-negative cells are resistant to apoptosis induced by these genotoxic agents despite activation of the Atr-Chk1 pathway (12, 13). The above proteins were not detected by this two-dimensional PAGE and MALDI-TOF/MS analysis possibly because differences in protein modification (e.g., phosphorylation and dephosphorylation) or protein structure do not necessarily cause significant mobility differences in two-dimensional PAGE gels. Proteins that were identified by two-dimensional PAGE and MALDI-TOF/MS in these experiments did not seem necessarily to be directly involved in Fhit tumor suppressor functions, although Ad-*FHIT*-wt infection (MOI 25) induced a substantial percentage of apoptosis after 120 hours after infection, a function we consider to be a Fhit suppressor function. However, the cells were collected 72 hours after viral infection not only to avoid contamination with apoptotic cells but also to provide clues to mechanisms of Fhit tumor suppression relatively early in the process. Thus, we consider that down-regulation of cyclophilin A is one of the earliest events in Fhit-induced proapoptotic activity, a manifestation of tumor suppressor activity in H1299 cells.

Transitions between cell cycle phases are tightly regulated, and checkpoints during cell cycle progression allow the cell to determine whether all is well before proceeding to the next cell cycle phase (27). Common to all the regulatory transitions of the cell cycle is the ubiquitous second messenger, Ca^{2+}, and the universally important Ca^{2+} intracellular receptors, calmodulin and calcineurin. Calcineurin, a heterodimeric molecule composed of a catalytic A subunit and a Ca^{2+}-binding regulatory B subunit, activates reentry into the cell cycle by up-regulating cyclin D1 and Cdk4 expression in the late G_1 phase (28-30). On the other hand, cyclophilin A is ubiquitously distributed in tissue, and the cyclophilin A/cyclosporine A complex has numerous known activities in cell growth, differentiation, transcriptional control, and cell signaling (28). In particular, the cyclophilin A/cyclosporine A complex is known to inhibit calcineurin activity and block cell proliferation; cyclosporine A treatment alone has been reported to inhibit cell proliferation (28, 31), but overexpression of cyclophilin A has been reported in human cancers by proteome analyses (32-35). Indeed, cyclosporine A is unable to inhibit calcineurin activity at high concentrations of cyclophilin A; cyclosporine A treatment induced a G_1 arrest in pancreatic acinar cells, but excess cellular cyclophilin A activates calcineurin (36). Howard et al. established stable RNA interference–mediated knockdown of cyclophilin A in human non–small lung cancer cells and found that knockdown of

Published OnlineFirst August 2, 2006; DOI: 10.1158/1541-7786.MCR-06-0060

cyclophilin A caused significant tumor cell growth suppression and induction of apoptosis *in vitro* and *in vivo* (37). In the current study, the levels of cyclin D1 and Cdk4 were indeed up-regulated by treatment with cyclophilin A presumably as a result of depletion of the cyclosporine A pool in cells and promotion of cyclin D1 synthesis by calcineurin (38). Our findings in this study may support the possibility that Fhit-mediated down-regulation of cyclophilin A inactivates calcineurin function and consequently suppresses cyclin D1 and Cdk4 protein synthesis (Fig. 6).

Further investigation will be required to define the mechanism by which Fhit down-modulates of cyclophilin A expression and effects on calcineurin activity. Cyclophilin A has been reported to enhance cell proliferation by activating Erk1/2 (p42/p44) and c-Jun NH_2-terminal kinase in vascular smooth muscle cells and endothelial cells (39, 40). Furthermore, cyclophilin A is known to modulate the activity of the Sin3-Rpd3 histone deacetylase complex, which cause mitotic arrest (41). Taken together, the demonstration of possible involvement of cyclophilin A in Fhit-deficient human lung cancers may provide new insights into the molecular mechanisms underlying carcinogenesis due to Fhit loss and prevention therapy due to Fhit replacement.

Materials and Methods

Cell Culture and Treatment

H1299 human lung carcinoma cells (lacking Fhit expression) obtained from the American Type Culture Collection (Manassas,

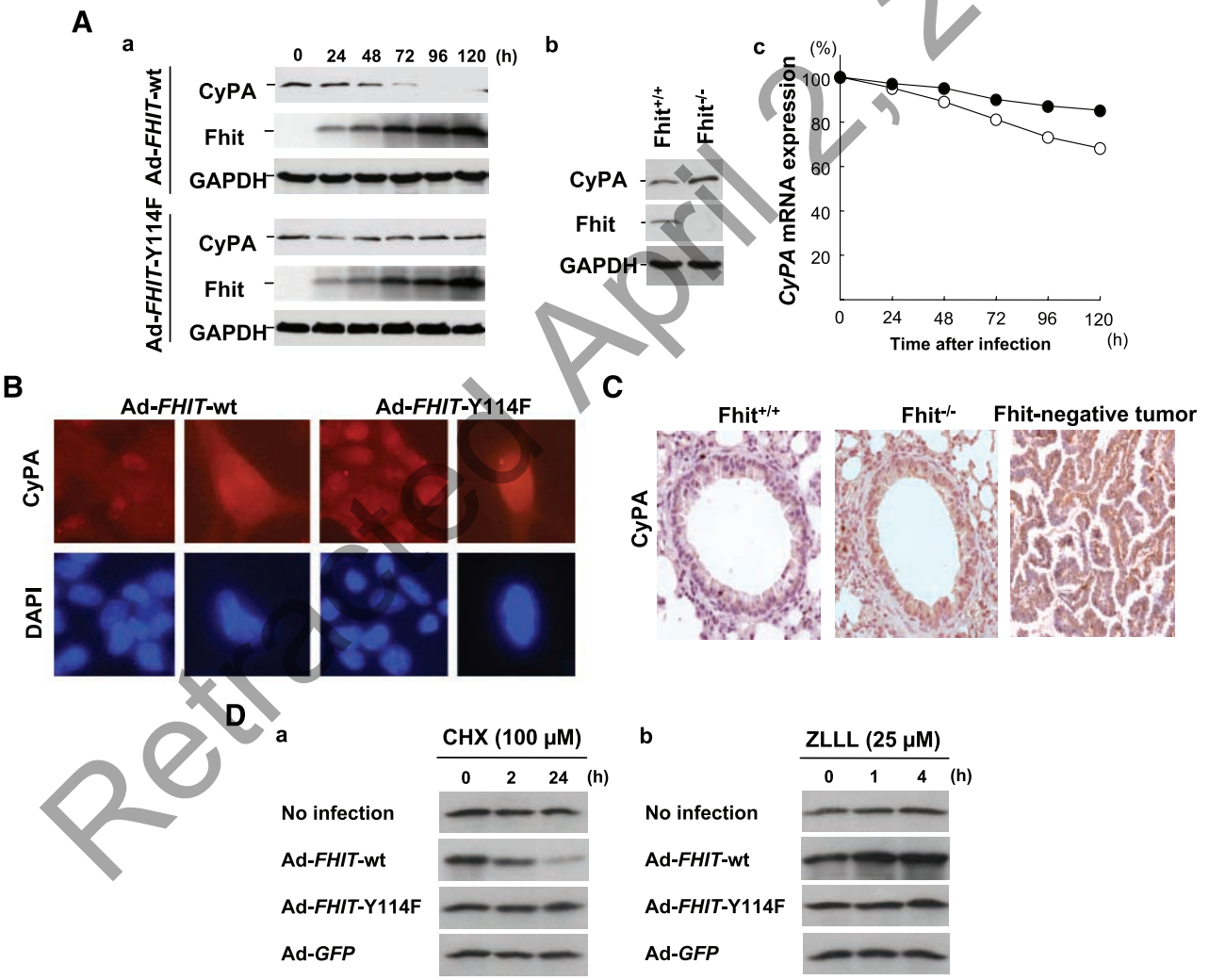

FIGURE 3. Down-regulation of cyclophilin A expression by wild-type Fhit. **A.** Time course analysis of decreased levels of cyclophilin A (*CyPA*) expression in H1299 cells after Ad-*FHIT*-wt infection (**a**) and comparison of basal levels of cyclophilin A expression in $Fhit^{+/+}$ and $Fhit^{-/-}$ mouse kidney cells (**b**). Anti-GAPDH antibody was used for loading control. **c,** results of quantitative real-time reverse transcription-PCR analysis of *cyclophilin A* mRNA expression. Levels of *cyclophilin A* mRNA expression before infection with adenoviruses are considered to be 100%. The cells were infected with Ad-*FHIT*-wt and Ad-*FHIT*-Y114F, respectively (MOI 25), and total RNAs isolated from these cells were used. Expression levels of *cyclophilin A* mRNA were calculated according to the $2^{-\Delta\Delta Ct}$ method as described in the text. ○, Ad-*FHIT*-wt; ●, Ad-*FHIT*-Y114F. **B.** Immunofluorescent detection of cyclophilin A expression. H1299 cells were infected with Ad-*FHIT*-wt and Ad-*FHIT*-Y114F, respectively. Cells were fixed 48 hours after infection. **C.** Immunohistochemical analysis of cyclophilin A expression in $Fhit^{+/+}$ and $Fhit^{-/-}$ mouse bronchial epithelia as well as Fhit-negative mouse lung adenocarcinoma tissues. **D.** Western blot analyses of cyclophilin A after treatment with cycloheximide (*CHX*; **a**) and Z-Leu-Leu-Leu-al (*ZLLL*; **b**). Experiments were done at least thrice.

Published OnlineFirst August 2, 2006; DOI: 10.1158/1541-7786.MCR-06-0060

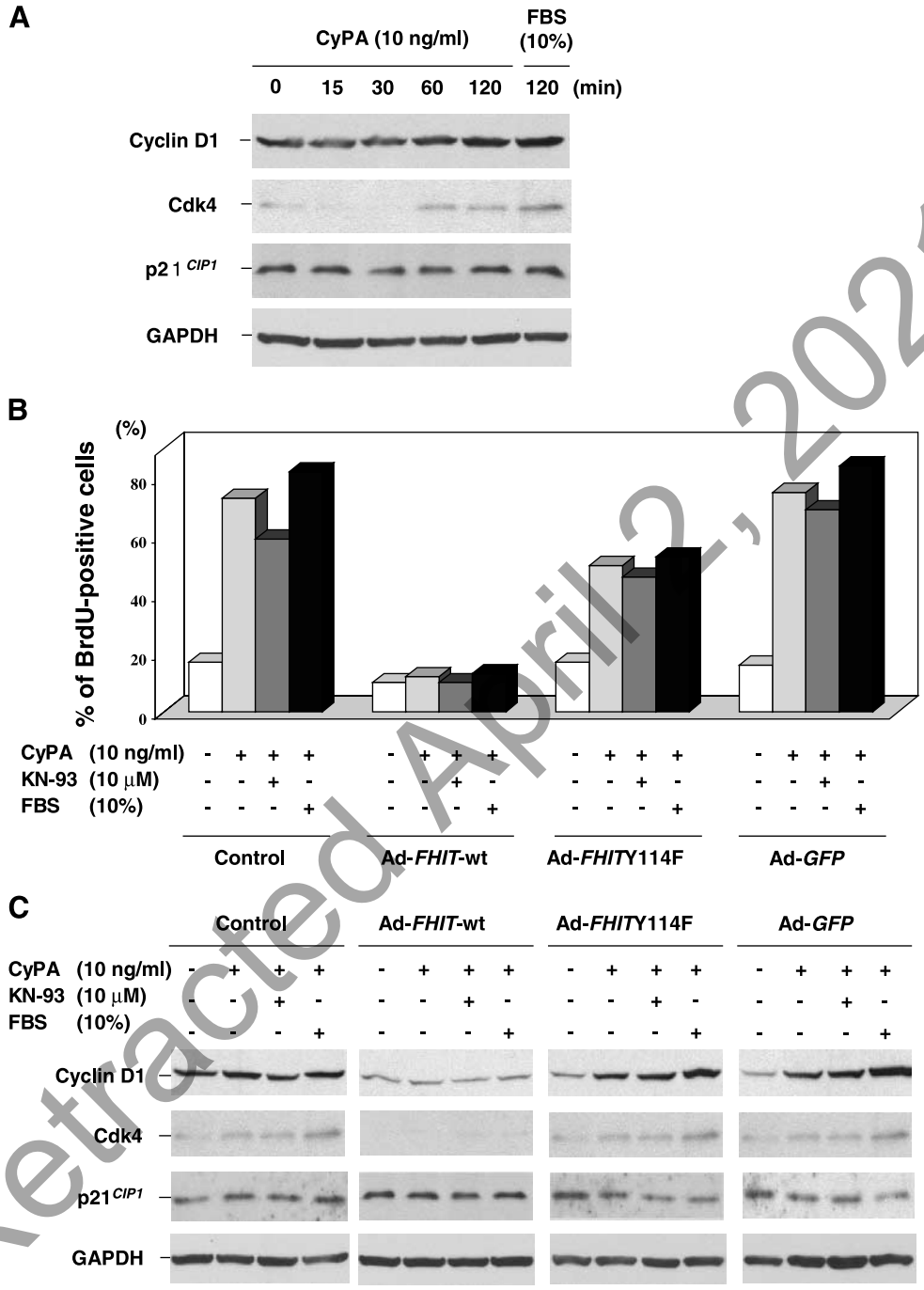

FIGURE 4. Cyclophilin A–mediated cell cycle progression in H1299 cells. **A.** Western blot of cyclin D1, Cdk4, and p21^{CIP1} cell cycle regulators after cyclophilin A treatment. Accumulation of cyclin D1 and induction of Cdk4 expression were detected 60 minutes after treatment with cyclophilin A. **B.** Results of BrdUrd incorporation analysis. After incubation of the cells in serum-free medium for 48 hours, H1299 cells were infected with Ad-*FHIT*-wt, Ad-*FHIT*-Y114F, or Ad-*GFP* (MOI 25) 24 hours before cyclophilin A stimulation. KN-93 Ca^{2+}/calmodulin-dependent kinase inhibitor was also used to inhibit Ca^{2+}/calmodulin-mediated G_1-S transition. As control, percentages of BrdUrd-positive cells in the presence or absence of fetal bovine serum were also counted. **C.** Effects of cyclophilin A on cyclin D1, Cdk4, and p21^{CIP1} cell cycle regulators at late G_1. Effect of cyclophilin A, KN-93, and fetal bovine serum on cells synchronized at late G_1 phase.

VA) and mouse kidney cells from Fhit$^{+/+}$ and Fhit$^{-/-}$ cells, respectively, were maintained in MEM supplemented with 10% fetal bovine serum (Sigma-Aldrich, St. Louis, MO), 100 units/L penicillin, and 100 μg/L streptomycin. Human recombinant cyclophilin A (Biomol, Plymouth Meeting, PA), cyclosporine A (Sigma-Aldrich), cycloheximide (Sigma-Aldrich), Z-Leu-Leu-Leu-al (Sigma-Aldrich), and KN-93 Ca^{2+}/calmodulin-dependent kinase inhibitor (Chemicon, Temecula, CA) were used in this study.

Published OnlineFirst August 2, 2006; DOI: 10.1158/1541-7786.MCR-06-0060

Gene Transduction with Recombinant FHIT-Expressing Adenoviruses

Adenoviruses carrying human recombinant wild-type (Ad-*FHIT*-wt) and Y114 mutant *FHIT* substituted with phenylalanine (Ad-*FHIT*-Y114F) were used in this study (14, 20). Briefly, wild-type and mutant *FHIT* cDNA were cloned into the transfer vector pAdenoVator-CMV5-GFP (Qbiogene, Carlsbad, CA). After recombination with the construct AdenoVator ΔE1/E3, resulting vectors were transfected into HEK293 cells to package viruses. Single viral plaques were isolated and recombinant wild-type and mutant Fhit expression was determined by immunoblot analysis. Ad-*GFP* virus was used as a nonspecific control for gene transfer (Qbiogene). Virus titers were determined by absorbance measurement, MOI test, and tissue culture ID_{50} method. Cells were incubated with adenoviral aliquots at a desired MOI for 4 hours before addition of culture medium (>25 × volume of virus inoculum).

Cell Viability Test, Flow Cytometric Analysis, and BrdUrd Incorporation

For cell viability tests, 5×10^5 cells were infected with individual adenoviruses (MOI 0-200), harvested, stained with trypan blue, and counted with the ViCell cell counter (Beckman Coulter, Fullerton, CA). To analyze cellular DNA content, 5×10^5 cells were infected with recombinant adenovirus (MOI 25), and at 120 hours, cells were fixed in 70% methanol, treated with RNase A, and stained with propidium iodide. For quantification of cells positive for active (cleaved) caspase-3, cells were washed, fixed, permeabilized, and stained with phycoerythrin-conjugated monoclonal anti-active caspase-3 (BD Biosciences, San Jose, CA). These analyses were done with a FACSCalibur cytometer (BD Biosciences). Experiments were repeated thrice. For the BrdUrd incorporation assay, cells were grown to 50% to 60% confluence on coverslips. After synchronization, cells were incubated with 10 μmol/L BrdUrd (Sigma-Aldrich) for 2 hours and fixed in Carnoy's fixative (3 parts methanol:1 part glacial acetic acid). After DNA denaturation with 2 N HCl, mouse anti-BrdUrd (Invitrogen, Carlsbad, CA) and Texas red–conjugated anti-mouse IgG antibodies detected BrdUrd-positive cells. Cell nuclei were stained with 4′,6-diamidino-2-phenylindole (Vector Laboratories, Burlingame, CA). Fluorescent cells were visualized by fluorescence microscopy.

Two-Dimensional PAGE and Protein Identification by MALDI-TOF and MS

H1299 cells (1×10^6) infected with Ad-*FHIT*-wt or Ad-*FHIT*-Y114F were lysed in sample buffer containing 7 mol/L urea, 2 mol/L triourea, 4% CHAPS, 2 mmol/L tributyl phosphine, and 0.2% BioLyte 3/10 ampholytes (Bio-Rad, Hercules, CA). The crude cell homogenate was sonicated and centrifuged at 10,000 × *g* for 10 minutes. Immobilized pH gradient strips (11 cm) with pH range 3 to 10 were hydrated overnight in sample buffer containing 200 μg total protein. After isoelectric focusing, using Protean Cell (Bio-Rad), proteins were separated in the second dimension by 8% to 16% gradient SDS-PAGE for 1 hour at 200 V. All gels were run thrice, stained with colloidal Coomassie blue (Pierce, Rockford, IL), and scanned with Versadoc 3000 image system (Bio-Rad). Gel images were captured with an 800 GS scanner (Bio-Rad) and analyzed using PDQuest software (Bio-Rad) by the total protein density in each of the gel images. Protein spots were quantified after normalization for total protein on the gel. For statistical analyses, the average results of the triplicates were calculated and the resulting values were used as independent data points in statistical analyses (Student's *t* test).

MS was carried out in the Ohio State University Davis Heart and Lung Research Institute Proteomics Core Laboratory. We attempted to identify proteins only from spots that were consistently reduced or induced at least 4-fold in all comparative gels. The protein spots were transferred to the MassPrep station (Perkin-Elmer, Wellesley, MA) for automated in-gel protein digestion following the protocol included with the WinPREP Multiprobe II software (Perkin-Elmer). Briefly, gel pieces were destained and then reduced with DTT. After incubation with iodoacetamide, gels were washed and dehydrated with acetonitrile. In-gel digestion of the extracted

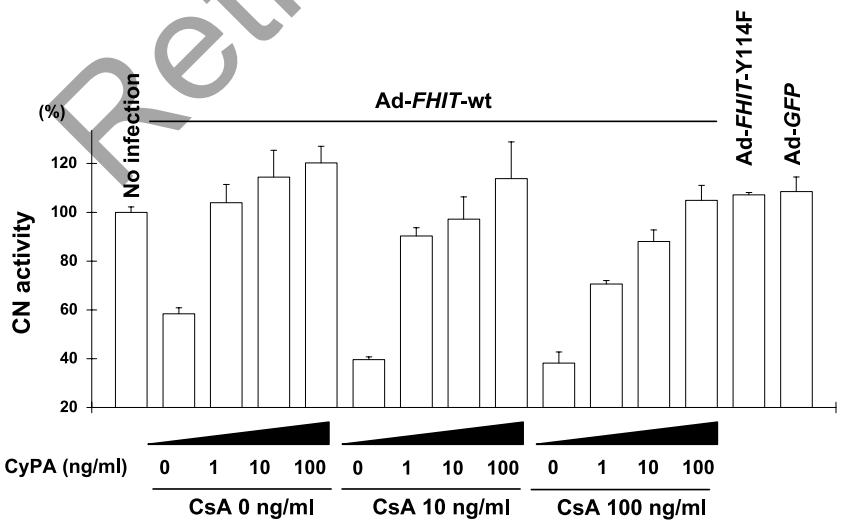

FIGURE 5. Results of calcineurin phosphatase activity in H1299 cells. After viral infection, cells were stimulated with or without cyclophilin A and/or cyclosporine A (*CsA*) treatment. Phosphatase activity of calcineurin (*CN*) was measured by Biomol Green Calcineurin Assay kit as described in the text.

Published OnlineFirst August 2, 2006; DOI: 10.1158/1541-7786.MCR-06-0060

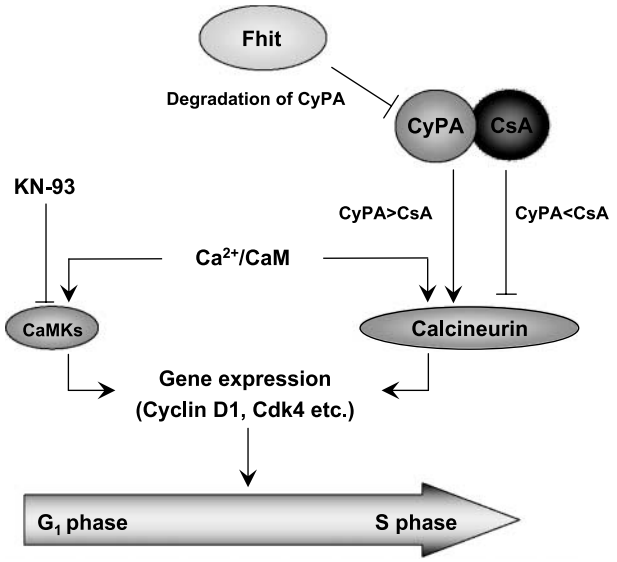

FIGURE 6. Proposed model for Fhit-mediated suppression of Ca^{2+}/calmodulin-dependent cell cycle progression by cyclophilin A down-modulation. Activation of calcineurin and Ca^{2+}/calmodulin-dependent kinase up-regulates transcription of cell cycle regulators, including cyclin D1 and Cdk4, resulting in G_1-S transition. The cyclophilin A/cyclosporine A complex negatively regulates the activity of calcineurin, and cyclosporine A treatment (cyclophilin A < cyclosporine A) also suppresses calcineurin, resulting in G_1 arrest. However, at high concentrations of cyclophilin A (cyclophilin A > cyclosporine A), cyclosporine A is unable to inhibit calcineurin activity. Fhit decreases the level of cyclophilin A expression presumably suppressing calcineurin function and Ca^{2+}/calmodulin-dependent cell cycle transition at late G_1.

proteins was carried out with 6 μg/mL trypsin in 50 mmol/L ammonium bicarbonate. The digested peptides were extracted with a mixture of 1% formic acid/2% acetonitrile and applied onto a stainless steel MALDI plate (Waters, Milford, MA). MS of the resulting peptides was recorded on the MALDI-TOF spectrometer (Waters) in reflectron mode. Resulting peptides were matched with their corresponding proteins with ProFound (http://prowl.rockefeller.edu/profound_bin/WebProFound.exe?FORM=1/) by searching the National Center for Biotechnology Information database (http://www3.ncbi.nlm.nih.gov/).

Western Blot Analysis and Immunohistochemistry

Samples were extracted in cell lysis buffer containing 50 mmol/L Tris-HCl (pH 7.4), 125 mmol/L NaCl, 0.1% Triton X-100, 5 mmol/L EDTA, 1% (v/v) protease inhibitor cocktail (Sigma-Aldrich), and 1% (v/v) phosphatase inhibitor cocktail (Sigma-Aldrich). Total protein (40 μg) was separated on 10% or 12% polyacrylamide gels (Bio-Rad) and transferred to Hybond-C membrane (Amersham Biosciences, Piscataway, NJ). Membranes were probed with antisera against Fhit (20), ANXA2 (Santa Cruz Biotechnology, Santa Cruz, CA), cyclophilin A, HSP70 (Santa Cruz Biotechnology), CAII (Santa Cruz Biotechnology), cyclin D1 (Neomarkers, Fremont, CA), Cdk4 (Transduction Laboratories, San Jose, CA), and $p21^{CIP1}$ (Neomarkers). As controls, antisera against GFP (Invitrogen) and glyceraldehyde-3-phosphate dehydrogenase (GAPDH; Calbiochem, San Diego, CA) antibodies were used. After probing with appropriate secondary anti-rabbit or anti-mouse IgG conjugated to horseradish peroxidase (Invitrogen), signals were detected by chemiluminescence substrate.

Formalin-fixed and paraffin-embedded mouse lung tissues from $Fhit^{+/+}$ and $Fhit^{-/-}$ mice as well as Fhit-deficient mouse lung adenocarcinoma tissues were used for immunohistochemical analyses. Antisera used for Western blot analysis were also suitable for immunohistochemistry. A modified version of the immunoglobulin enzyme bridge technique was used (20). Briefly, deparaffinized tissue sections were immersed in methanol containing 0.03% hydrogen peroxide for 30 minutes to block endogenous peroxide activity after autoclave pretreatment in citrate buffer to retrieve the antigenicity. After blocking the nonspecific antibody binding sites, the sections were treated at room temperature with appropriate antiserum. Peroxide staining was done for 2 to 5 minutes using a solution of 3,3′-diaminobenzidine in 50 mmol/L Tris-HCl (pH 7.5) containing 0.001% hydrogen peroxide (Chemicon). Sections were counterstained with hematoxylin.

Quantitative Real-time Reverse Transcription-PCR

Total RNAs were isolated from H1299 cells infected with Ad-*FHIT*-wt, Ad-*FHIT*-Y114F, or Ad-*GFP*, respectively, using the RNeasy Mini kit (Qiagen, Hilden, Germany). Quantitative real-time reverse transcription-PCR analyses were done using the iCycler multicolor real-time PCR detection system (Bio-Rad) and the QuantiTect SYBR Green Reverse Transcription-PCR kit (Qiagen) as described elsewhere (20). The primer sets used in this study were *cyclophilin A* forward 5′-TAAAGCATACGGGTCCTGGC-3′ and reverse 5′-TCGAGTTGTCCACAGTCAGC-3′ and *GAPDH* forward 5′-GAAGGTGAAGGTCGGAGT-3′ and reverse 5′-GAAGATGGTGATGGGATTTC-3′. After an initial 30-minute incubation at 50°C and 15-minute denaturation at 95°C, the following cycling conditions (45 cycles) were used: denaturation at 94°C for 15 seconds, annealing at 60°C for 15 seconds, and elongation at 72°C for 15 seconds. All experiments were done in triplicate. Using *GAPDH* as a housekeeping gene, the expression levels of *cyclophilin A* mRNA were calculated as described (20). The Ct values of triplicate reverse transcription-PCR were averaged for each gene in each cDNA sample. For each tissue sample assayed, the average Ct value for the *cyclophilin A* gene was subtracted from the average Ct value of the *GAPDH* gene to obtain the ΔCt value. The ΔCt value of the reference sample was subtracted to obtain the ΔΔCt value. No significant change was found in the cells infected with Ad-*GFP* (data not shown).

Calcineurin Phosphatase Activity Assay

Calcineurin phosphatase activity was analyzed with the Biomol Green Calcineurin Assay kit in accordance with the manufacturer's instructions. In brief, cell lysates were centrifuged at 10,000 × *g* and desalted using a P6 DG resin to remove excess phosphate and other nucleotides. Desalted samples were added to assay buffer, containing RII phosphopeptide as a substrate for calcineurin, in triplicate. Samples were then incubated at 30°C for 10 minutes, after which 100 μL Biomol Green reagent were added to stop the reaction. The samples were then incubated at room temperature for 30 minutes to allow color development, and the absorbance at

Published OnlineFirst August 2, 2006; DOI: 10.1158/1541-7786.MCR-06-0060

620 nm (A_{620}) was determined for each sample. Calcineurin-specific phosphatase activity was determined by subtracting the A_{620} of samples with total phosphatase activity from the A_{620} of samples in the presence of EGTA.

Acknowledgments

We thank Drs. Arun K. Tewari and Jeff Cotrill (Proteomics Core Laboratory, Davis Heart and Lung Research Institute, Ohio State University) for expert assistance with proteomic analysis.

References

1. Sekido Y, Fong KM, Minna JD. Progress in understanding the molecular pathogenesis of human lung cancer. Biochim Biophys Acta 1998;1378:21–59.

2. Ohta M, Inoue H, Cotticelli MG, et al. The *FHIT* gene, spanning the chromosome 3p14.2 fragile site and renal carcinoma-associated t(3;8) breakpoint, is abnormal in digestive tract cancers. Cell 1996;84:587–97.

3. Sozzi G, Veronese ML, Negrini M, et al. The *FHIT* gene 3p14.2 is abnormal in lung cancer. Cell 1996;85:17–26.

4. Huebner K, Garrison PN, Barnes LD, Croce CM. The role of the *FHIT/FRA3B* locus in cancer. Annu Rev Genet 1998;32:7–31.

5. Croce CM, Sozzi G, Huebner K. Role of FHIT in human cancer. J Clin Oncol 1999;17:1618–24.

6. Kuroki T, Trapasso F, Yendamuri S, et al. Allelic loss on chromosome 3p21.3 and promoter hypermethylation of semaphorin 3B in non-small cell lung cancer. Cancer Res 2003;63:3724–8.

7. Iliopoulos D, Guler G, Han SY, et al. Fragile genes as biomarkers epigenetic control of *WWOX* and *FHIT* in lung, breast and bladder cancer. Oncogene 2005;24:1625–33.

8. Huebner K, Croce CM. Cancer and the *FRA3B/FHIT* fragile locus: it's a HIT. Br J Cancer 2003;88:1501–6.

9. Zanesi N, Fidanza V, Fong LY, et al. The tumor spectrum in *FHIT*-deficient mice. Proc Natl Acad Sci U S A 2001;98:10250–5.

10. Fujishita T, Doi Y, Sonoshita M, et al. Development of spontaneous tumors and intestinal lesions in *Fhit* gene knockout mice. Br J Cancer 2004;91:1571–4.

11. Zanesi N, Mancini R, Sevignani C, et al. Lung cancer susceptibility in Fhit-deficient mice is increased by Vhl haploinsufficiency. Cancer Res 2005;65:6576–82.

12. Ottey M, Han SY, Druck T, et al. Fhit-deficient normal and cancer cells are mitomycin C and UVC resistant. Br J Cancer 2004;91:1669–77.

13. Hu B, Han SY, Wang X, et al. Involvement of the Fhit gene in the ionizing radiation-activated ATR/CHK1 pathway. J Cell Physiol 2005;202:518–23.

14. Dumon KR, Ishii H, Vecchione A, et al. Fragile histidine triad expression delays tumor development and induces apoptosis in human pancreatic cancer. Cancer Res 2001;61:4827–36.

15. Ishii H, Dumonm KR, Vecchione A, et al. Effect of adenoviral transduction of the fragile histidine triad gene into esophageal cancer cells. Cancer Res 2001;61:1578–84.

16. Roz L, Gramegna M, Ishii H, Croce CM, Sozzi G. Restoration of *fragile histidine triad* (*FHIT*) expression induces apoptosis and suppresses tumorigenicity in lung and cervical cancer cell line. Proc Natl Acad Sci U S A 2002;99:3615–20.

17. Sevignani C, Calin GA, Cesari R, et al. Restoration of *fragile histidine triad* (*FHIT*) expression induces apoptosis and suppresses tumorigenicity in breast cancer cell lines. Cancer Res 2003;63:1183–7.

18. Dumon KR, Ishii H, Fong LY, et al. *FHIT* gene therapy prevents tumor development in Fhit-deficient mice. Proc Natl Acad Sci U S A 2001;98:3346–51.

19. Pekarsky Y, Garrison PN, Palamarchuk A, et al. Fhit is a physiological target of the protein kinase Src. Proc Natl Acad Sci U S A 2004;101:3775–9.

20. Semba S, Trapasso F, Fabbri M, et al. Fhit modulation of the Akt-survivin pathway in lung cancer cells: Fhit-tyrosine 114 (Y114) is essential. Oncogene 2006;25:2860–72.

21. Schneider G, Oswald F, Wahl C, Greten FR, Adler G, Schmid RM. Cyclosporin inhibits growth through the activating transcription factor/camp-responsive element-binding protein binding site in the cyclin D1 promotor. J Biol Chem 2002;277:43599–607.

22. Baksh S, Wildlund HR, Frazer-Abel AA, et al. NFATc2-mediated repression of cyclin-dependent kinase 4 expression. Mol Cell 2002;10:1071–81.

23. Baksh S, DeCaprio JA, Burakoff SJ. Calcineurin regulation of the mammalian G_0-G_1 checkpoint element, cyclin dependent kinase 4. Oncogene 2000;19:2820–7.

24. Rohr UP, Rehfeld N, Geddert H, et al. Prognostic relevance of fragile histidine triad protein expression in patients with small cell lung cancer. Clin Cancer Res 2005;11:180–5.

25. Burke L, Khan MA, Freedman AN, et al. Allelic deletion analysis of the *FHIT* gene predicts poor survival in non-small cell lung cancer. Cancer Res 1998;58:2533–6.

26. Guler G, Uner A, Guler N, et al. The *fragile genes FHIT* and *WWOX* are inactivated coordinately in invasive breast carcinoma. Cancer 2004;100:1605–14.

27. Hanahan D, Weinberg RA. The hallmarks of cancer. Cell 2000;100:57–70.

28. Kahl CR, Means AR. Regulation of cell cycle progression by calcium/calmodulin-dependent pathways. Endocr Rev 2003;24:719–36.

29. Galat A. Peptidylproline *cis-trans*-isomerases: immunophilins. Eur J Biochem 1993;216:689–707.

30. Klee CB, Ren H, Wang X. Regulation of the calmodulin-stimulated protein phosphatase, calcineurin. J Biol Chem 1998;273:13367–70.

31. Guerini D. Calcineurin: not just a simple protein phosphatase. Biochem Biophys Res Commun 1997;235:271–5.

32. Howard BA, Zheng Z, Campa MJ, et al. Translating biomarkers into clinical practice: prognostic implications of cyclophilin A and macrophage migratory inhibitory factor identified from protein expression profiles in non-small cell lung cancer. Lung Cancer 2004;46:313–23.

33. Campa MJ, Wang MZ, Howard B, Fitzgerland MC, Patz EF, Jr. Protein expression profiling identifies macrophage migration inhibitory factor and cyclophilin a as potential molecular targets in non-small cell lung cancer. Cancer Res 2003;63:1652–6.

34. Fratelli M, Demol H, Puype M, et al. Identification of proteins undergoing glutathionylation in oxidatively stressed hepatocytes and hepatoma cells. Proteomics 2003;3:1154–61.

35. Shen J, Person MD, Zhu J, Abbruzzese JL, Li D. Protein expression profiles in pancreatic adenocarcinoma compared with normal pancreatic tissue and tissue affected by pancreatitis as detected by two-dimensional gel electrophoresis and mass spectrometry. Cancer Res 2004;64:9018–26.

36. Kung L, Halloran PF. Immunophilins may limit calcineurin inhibition by cyclosporine and tacrolimus at high drug concentrations. Transplantation 2000;70:327–35.

37. Howard BA, Furumai R, Campa MJ, et al. Stable RNA interference-mediated suppression of cyclophilin A diminishes non-small-cell lung tumor growth *in vivo*. Cancer Res 2005;65:8853–60.

38. Kahl CR, Means AR. Calcineurin regulates cyclin D1 accumulation in growth-stimulated fibroblasts. Mol Biol Cell 2004;15:1833–42.

39. Jin ZG, Melaragno MG, Liao DF, et al. Cyclophilin A is a proinflammatory cytokine that activates endothelial cells. Circ Res 2000;87:789–96.

40. Jin ZG, Lingu AO, Xie L, Wang M, Wong C, Berk BC. Cyclophilin A is a proinflammatory cytokine that activates endothelial cells. Arterioscler Thromb Vasc Biol 2004;24:1186–91.

41. Arevalo-Rodriguez M, Cardenas ME, Wu X, Hanes SD, Heitman J. Cyclophilin A and Ess1 interact with and regulate silencing by the Sin3-3 histone deacetylase. EMBO J 2000;19:3739–49.

Retraction: Protein Expression Profiling Identifies Cyclophilin A as a Molecular Target in Fhit-Mediated Tumor Suppression

This article (1) has been retracted at the request of the corresponding author, K. Huebner. Examination of the data uncovered unexpected similarities in certain figures in this study. In addition, data in several figures from this study appear to overlap with data previously published by the authors in an earlier *Oncogene* article (2). This information was communicated to the corresponding author, who was not able to locate the original data from 2005, but who agreed that there were aberrations in the data that could not be explained. Specifically:

- The same image seems to have been used to represent the GFP blot in Fig. 1Aa of this study (1) and the GFP blots in Fig. 1Ab of the *Oncogene* study (2).
- The Ad-FHIT-wt GAPDH blot and the Ad-FHIT-Y114F GAPDH blot in Fig. 3A of this study (1) seem to match, respectively, the first six lanes of the A549 GAPDH blot and the last six lanes of the H1299 GAPDH blot in Fig. 1Ab of the *Oncogene* study (2).
- In Figure 4C of this study (1):
  - CDK4 blots in the first, third, and fourth columns seem to share a common origin.
  - The $p21^{CIP1}$ blots in the first, third, and fourth columns seem to share a common origin. There are differences in the intensity of signal between these three blots, but the similarity of the band patterns suggests that these may represent multiple different exposures from the same blot.
  - The first two lanes of the $p21^{CIP1}$ blot in the second column seem to match the first two lanes of the $p21^{CIP1}$ blot in Fig. 4A. Similarly, the last two lanes of the $p21^{CIP1}$ blot in the second column of Fig. 4C seem to match the fourth and fifth lanes of the $p21^{CIP1}$ blot in Fig. 4A.

Given the potential issues outlined herein and that the original data are no longer available to correct the record, the corresponding author has requested that the study be retracted. The corresponding author apologizes to the scientific community and regrets any inconveniences or challenges resulting from the publication and subsequent retraction of this article.

References

1. Semba S, Huebner K. Protein expression profiling identifies cyclophilin A as a molecular target in Fhit-mediated tumor suppression. Mol Cancer Res 2006;4:529–38.
2. Semba S, Trapasso F, Fabbri M, McCorkell KA, Volinia S, Druck T, et al. Fhit modulation of the Akt-survivin pathway in lung cancer cells: Fhit-tyrosine 114 (Y114) is essential. Oncogene 2006;25:2860–72.

Published online April 1, 2021.
Mol Cancer Res 2021;19:740
doi: 10.1158/1541-7786.MCR-21-0107

AACR American Association for Cancer Research

Molecular Cancer Research

Protein Expression Profiling Identifies Cyclophilin A as a Molecular Target in Fhit-Mediated Tumor Suppression

Shuho Semba and Kay Huebner

Mol Cancer Res 2006;4:529-538. Published OnlineFirst August 2, 2006.